International Journal of Innovative Technology and Exploring Engineering (IJITEE)
ISSN: 2278-3075 (Online), Volume-8 Issue-4, February 2019

Analysis of Dermoscopic Images using Multiresolution Approach

K.S Rajasekhar, T Ranga Babu

Abstract*: Abnormal growth of cells in any part of the body is called cancer. Cancer that is formed on skin is called skin cancer. Life span of a cancer patient can be increased by the early detection of tumor part. This paper deals with classification of dermoscopic images, i.e. benign or malignant based on coefficients extracted from multiresolution analysis based wavelet functions and tetrolet transform. Statistical texture features such as Mean, Standard Deviation, Kurtosis and Skewness are calculated from the coefficients of the multiresolution transfroms. The Gray Level Co-occurence Matrix(GLCM) is calculated for the dermoscopic images from which features such as homogenity, energy and entropy are calculated. In addition to these shape features are also taken into consideration. K-Nearest Neighbor(KNN) classifier is used for classification of dermoscopic images. In this work, dermoscopic images are obtained from the International Skin Imaging Archive (ISIC). The performance of the system is evaluated using accu-racy, sensitivity and specificity. The area under the curve(AUC) demonstrates the superiority of tetrolet transform.

Index Terms*: Dermoscopic images, Texture features, GLCM features, Shape features, KNN classifier, Accuracy, Sensitivity, Specificity and AUC.

I. INTRODUCTION

The abnormal growth of skin cells is called skin cancer which is caused in the areas exposed tosun rays. The different types of skin cancer are Ac-tinic Keratoses, Basal Cell Carcinoma, Squamous Cell Carcinoma and Melanoma [1]. Many computer aided diagnostic systems have been developed for early diagnosis of skin cancer. Basal Cell carcinoma or Squamous cell carcinoma occur in 40 to 50% of Americans who are aged greater than 65. Melanoma is the most deadly skin cancer that can be cured if detected at an earlier stage. Enormous work have been done for the detection of melanoma skin cancer at an early stage. Sheha, Mariam A et. al., [2] have detected melanoma using GLCM features which are further classified using multi-layer perceptron achieving 100% for the training set and 92% for the test set. The local fractal and texture features are used for automatic detection of malignancy of skin lesions by Dobrescu, Radu, et. al., [3] achieving efficient results.

Celebi M Emre et al., [4] have classified dermoscopy images using both color and texture features. These color and texture features are opti-mized using relief algorithm which are then clas-sified using linear SVM achieving a specificity of 92.34% and sensitivity of 93.33%. Lau Ho Tak et. al., [5] have done early detection of skin cancer using DWT features which are classified using three layers back propagation neural network and auto-associative neural network achieving a recognition accuracy of 89.9% and 80.8% respectively.

Elgamal, Mahmoud et. al., [6] have done automatic skin cancer classification using DWT features which are reduced in dimension using PCA achieving classification of 95% and 97.5% based on feed-forward back propagation artificial neural network and KNN classification. Yuan, Xiaojing, et. al., [7] have done early detection of melanoma using SVM based texture classification achieving an accuracy 70% in determining the malignancy of any pixel within any given skin lesion image using 4th-order polynomial kernel. Yu, Lequan, et. al., [8] has done automated melanoma recognition using residual networks with softmax layer achieving AUC of 0.79. All the works from [2-8] are done on dermoscopic images which are obtained from general sources such as medical labs and hospitals.

In this work the dermoscopic images which are to be classified can be acquired from ISBI challenge 2016 of ISIC archive [9]. Table I depicts the previous works done on ISIC Archive database. The dermoscopic images need to be first analyzed for risk i.e benign and malignant as shown in Fig.1. The malignant images can further be classified into melanoma, basal cell carcinoma, squamous cell car-cinoma and nevus. Section 2 gives a brief introduc-tion about Tetrolet transform and Discrete wavelet transform. Section 3 gives description about the database and explains about the feature extraction. Section 4 presents the results for classification of dermoscopic images. Section 5 contains conclusions and future work.

II. OVERVIEW

A. Tetrolet Transform

Jens Krommweh et. al., [10] proposed Tetrolet transform based on Adaptive Haar wavelet trans-form that can be used to represent images effi-ciently. The basic support for Haar type wavelets are Tetrominoes, formed by connecting squares which are of equal size. Fig. 2 depicts the five basic shapes of tetrominoes, that are formed by taking into account 2-dimensional square data set. The rotations and reflections of the five different shapes addresses the tiling problem of the tetrominoes are show in Fig 3. when N is even tetrominies can cover each and every square of $[0,N]^2$. An optimum solution can be obtained by partitioning an image into 4X4 squares for efficient non overlapping coverage.

Manuscript published on 28 February 2019.
***Correspondence Author(s)
K.S Rajasekhar, ECE Department, Research Scholar, Acharya Nagarjuna University, Guntur, India.
Dr T.Ranga Babu, ECE Department, Professor, RVR &JC College of Engineering & Technology, Guntur, India

The low-pass and high-pass filters in a traditional Haar can be obtained by averaging sum and difference of each four typical values that are filed in a 2X2 square image $B_{p,q}$. The set $E = B_{0,0,\ldots,}B_{N/21,N/21}$ gives the dyadic partition of the image index set B. The pixels can be arranged into unique order by the bijective mapping £ that maps the four pixel pair of $B_{p,q}$ to the set {0,1,2,3}. The following equation describes the formation of a low pass part

$$a^1 = (a^1\,[p,q])_{p,q=0}^{\frac{N}{2}-1} \text{ with}$$

$$a^1\,[p,q] = \sum_{(p',q')\,\in B_{(p,q)}} \in [0, £(p',q')]a\,[p',q'] \quad (1)$$

and three high pass parts for $l = 0,1,2,3$

$$w_l^1 = (w_l^1\,[p,q])_{p,q=0}^{\frac{N}{2}-1} \text{ with}$$

$$w_l^1\,[p,q] = \sum_{(p',q')\,\in B_{(p,q)}} \in [0, £(p',q')]a\,[p',q'] \quad (2)$$

where the coefficients $l,m = 0,..3$ are entries from the Haar wavelet transform matrix.

$$W := (\in[r,s])_{r,s=0}^{3} = \frac{1}{2}\begin{bmatrix} 1 & 1 & 1 & 1 \\ 1 & 1 & -1 & -1 \\ 1 & -1 & 1 & 1 \\ 1 & -1 & -1 & 1 \end{bmatrix} \quad (3)$$

However the rigid blocking does not consider the local structure of the image by the dyadic squares $B_{p,q}$. The efficient representation of the local image geometry can be obtained by more tetromino segments

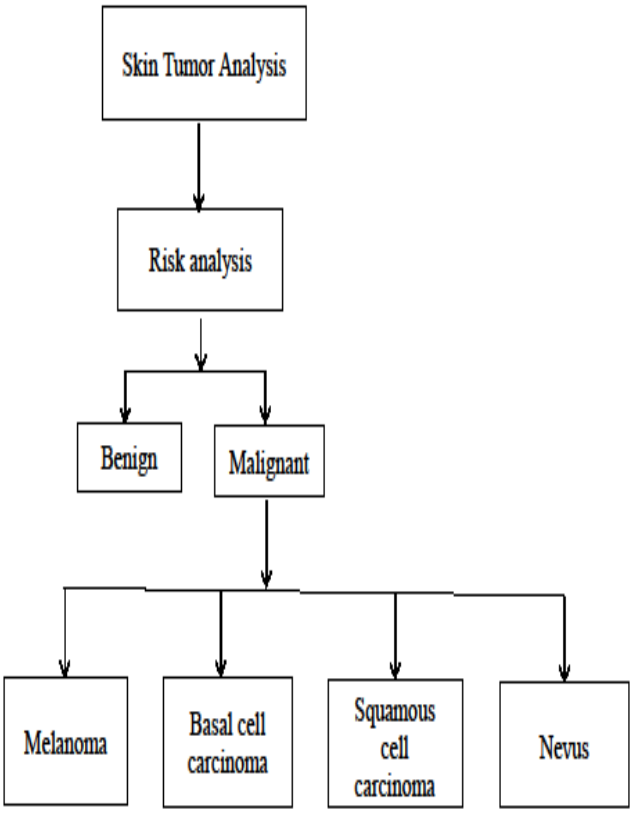

Fig. 1. Analysis of Dermoscopic Images

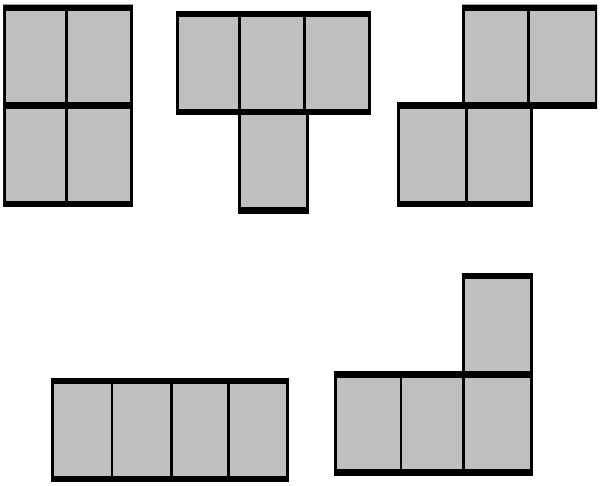

Fig. 2. Basic Shapes of Tetrominoes

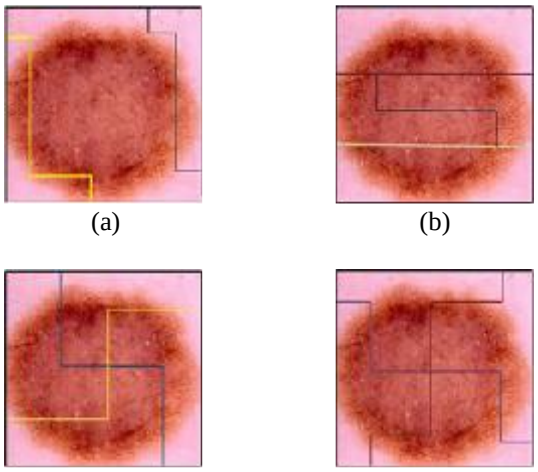

(a) (b) (c) (d)

Fig. 3. Fundamental tilings using Tetrominoes for Dermoscopic images

The Tetrolet decomposition algorithm can be described in detail by the following steps.

1. By considering the input image $B^0 = (B[p,q])_{p,q=0}^{N-1}$ with $N = 2^Q\ Q \in N$
2. The input image must be separated into $4X4$ blocks.
3. Each block should be formed by sparsest tetrolet representation..
4. The low-pass and high-pass coefficients of each square should be organised into a $2X2$ block.
5. The high-pass coefficients in each $2X2$ block should be accumulated, since they frame the Tetrolet coefficients.
6. Decomposition using steps 1-4 must be done for the low pass image.

Along these lines Tetrolet coefficients can be acquired for a dermoscopic image.

Table I Author Comparison

Published By:
Blue Eyes Intelligence Engineering
and Sciences Publication (BEIESP)

Sl. No	Author (Year)	Technique Used	No. of images	Accuracy	Sensitivity
1	Haenssle, H. A., et al.(2018) [11]	Deep convolution Neural Networks	100	AUC=0.82	88.9
2	Nazneen N Sultana et.al.(2018) [14]	Sparse coding and SVM	1279	83.09	NA
3	Lei Bi et.al.,(2017) [12]	Multistage Fully Convolution Neural Network	1279	90.51	92.17
4	Lequan Y U et.al.,(2017) [16]	Fusion of softmax and SVM classifier	1250	85.5	54.7
5	Lopez, Adria Romero, et. al.(2017) [17]	VGG Net convolutional neural network architecture	1279	81.33	78.66
6	Roberta B. Oliveira et.al., (2017) [18]	Ensemble classification model based on input feature manipulation	1104	91.3	91.8
7	Yi, Xin et.al., (2017) [19]	Generative Adversarial networks	140	0.424(Precision)	NA
8	Heydy Castillejos-Fernndez et.al.,(2017) [20]	Dull Razon algorithm for preprocessing Fuzzy Discrete wavelet transform for feature extraction , Multi agent ensemble of classifiers for classification	147	88	NA
9	Rahman et al.(2016) [13]	Non sub sampled contourlet transform Extreme learning machine	379	0.895	0.453
10	Majtner, Tomas.(2016) [21]	R-Surface and LBP features classified using SVM	900	0.826	0.533
11	Noel Codella et.al.,(2015) [15]	Deep Learning Sparse Coding and SVM	334	93.1	94.9

B. Discrete Wavelet Transform

Earlier work on images was done using Fourier transforms whose basis functions are sinusoids that provide only frequency information, which leads to loss in temporal information. The limitations in Fourier transform were overcome using wavelet transform dependent on tiny waves called wavelets of differing recurrence and con-strained length. Fine details in a signal can be obtained by using wavelets. To isolate fine details in a signal a very small amount of wavelets can be used, and to identify coarse details in a signal large amount of wavelets can be used. The different type of wavelets are Coiflet, Morlet, Daubechies, Haar etc. A more sparse representation of a signal may be generated by one particular wavelet than another, because of which different types of wavelets must be examined to identify the most suited for image classification

1. Two dimensional discrete wavelet transform:

The critical elements in a 2-dimensional wavelet transforms are one 2D scaling function $\psi(x,y)$ and three 2D wavelets $\psi^{h(x,y)}, \psi^{v(x,y)}, \psi^{d(x,y)}$. These scaling functions are composed of product of 1D scaling factor and corresponding wavelet ψ

$$\phi(x,y) = \phi(x)\phi(y) \quad (4)$$
$$\psi^{h(x,y)} = \psi(x)\phi(y) \quad (5)$$
$$\phi^{v(x,y)} = \phi(x)\psi(y) \quad (6)$$
$$\phi^{d(x,y)} = \phi(x)\phi(y) \quad (7)$$

Where ψ^h , ψ^v , ψ^d represents variations along the horizontal, vertical and diagonal directions. The scaled and translated basis functions are defined as

$$\phi_{j,m,n}(x,y) = 2^{\frac{1}{2}}\phi(2^j x - m, 2^j y - m) \quad (8)$$
$$\psi^i_{j,m,n}(x,y) = 2^{\frac{1}{2}}\psi^i(2^j x - m, 2^j y - m), i = H,V,D \quad (9)$$

Where index i identifies the directional wavelets in Eq.8 & 9.The discrete wavelet transform of function $f(x,y)$ of size $M\ X\ N$ is then

$$W_\phi(j_0,m,n) = \frac{1}{\sqrt{(MN)}}\sum_{x=0}^{M-1}\sum_{x=0}^{N-1} f(x,y)\phi_{j_0,m,n}(x,y) \quad (10)$$

$$W^i_\psi(j,m,n) = \frac{1}{\sqrt{(MN)}}\sum_{x=0}^{M-1}\sum_{x=0}^{N-1} f(x,y)\,\psi^i_{j_0,m,n}(x,y),, i = H,V,D \quad (11)$$

Published By:
Blue Eyes Intelligence Engineering
and Sciences Publication (BEIESP)

Where j_0 is an arbitrary starting scale and $W_\phi(j_0, m, n)$ coefficients

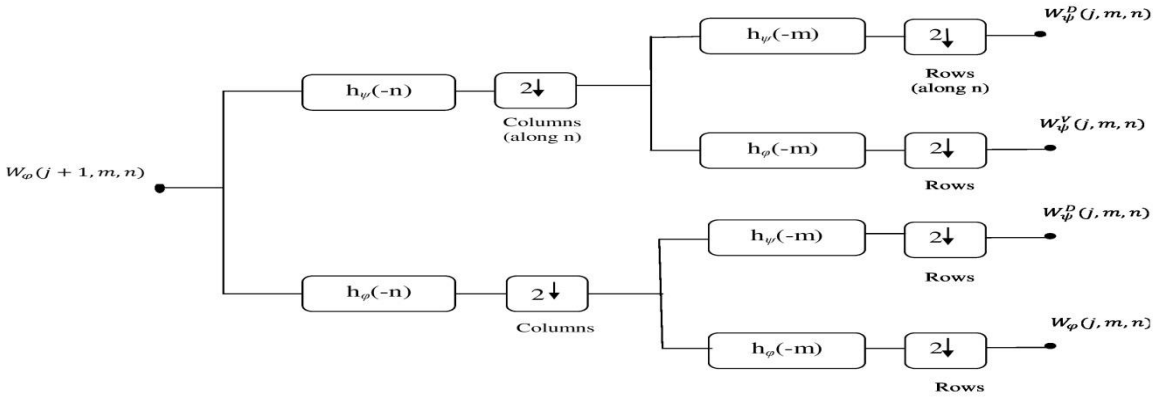

Fig 4. Analysis Filter Bank

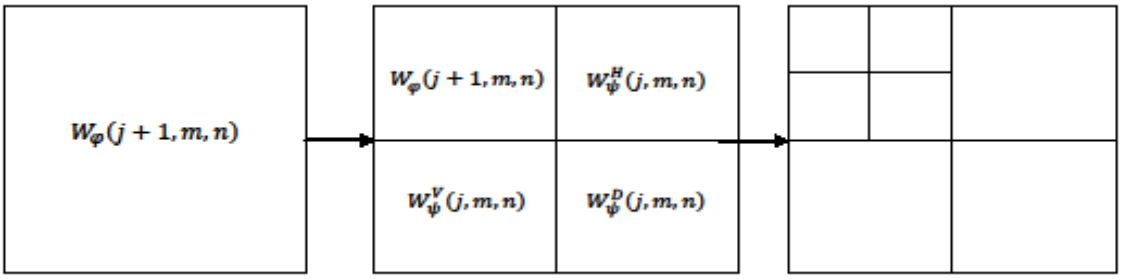

Fig 5. Three level decomposition

define an approximation of $f(x,y)$ at scale j_0. The $W_\psi^i(j,m,n)$coefficients add horizontal, vertical and diagonal details for scales $j \geq j_0$. Generally $j_0 = 1$ and $N = M = 2^J$so that $j = 0,1,2,..,J-1$ and $m,n = 0,1,2,\dots\dots,2^j - 1$. Analysis Filter bank can be shown in Fig 4.

Expanding $f(x,y)$ into numbers yields coefficients. By iterating the single scale filter bank, multi scale filter bank can be generated by approximation of the input to another filter. In two dimensional case $f(x,y)$ is used as input which decompose an image into four sub bands where as in three level decomposition it further decompose into sub bands with Low-Low(LL), Low-High(LH), High-Low(HL) and High-High(HH) as shown in Fig 5.

Multi resolution analysis can be done by using discrete wavelet transform. To represent an image into several sub images and analyzing them in the frequency domain, multiresolution analysis is used. While processing, texture extraction it is necessary to measure texture coefficients of neighborhood of different sizes using wavelet multiresolution transform which preserves the original image into sub bands that preserve high and low information.

III . METHODOLOGY

The methodology for work flow is as shown in Fig 6. Preprocessing is a fundamental component of any imaging modalities, whose main objective is to execute such procedures, which can convey the image to that quality, where it is reasonable to assist investigation and extraction of huge information. The tumors obtained from the database consist of noise acquired due to the scanners, tape artifacts and patient information. So preprocessing of the tumor images needs to be done prior to feature extraction. extraction is done to obtain the characteristics of an image. Several multiresolution approaches have been used to extract features from the dermoscopic images. A common approach after feature extraction is classification. Data analysis that can be used to extract models describing important data classes can be done by classification. The discrete, unordered labels can be predicted by classification. Training and testing are the two successive procedures in classification algorithms.

An exclusive definition of any class is done by training with classic features obtained from the training patterns and dividing them in the feature space in original training phase. In the consequent testing phase, the new input features obtained from testing data set are classified using these feature space. Therefore, sub-space class of each feature vector is determined by the classification problem. If the classes are specified apriori, then it is known as supervised classification otherwise it is known as unsupervised classification that depends on clustering algorithms to automatically divide the training data into prototype classes. In this work K-Nearest Neighbor Classifier is used for classifying the skin tumor images into benign and malignant.

Published By:
Blue Eyes Intelligence Engineering and Sciences Publication (BEIESP)

1) Dataset: The dataset for this work is taken from ISIC archive ISBI challenge 2016[13]. The data is in jpeg format which consists of 212 cases of skin cancer for testing 617 cases for training. First the images are subjected to prepossessing to remove noise and to obtain cropped Region of Interest(ROI) of size 256 X 256 which removes the pixel information and background which is not useful. Fig 7 shows malignant and benign images obtained from ISIC archive ISBI challenge 2016.

2) Feature Extraction*:* Feature extraction is an important technique to detect and isolate desired portions of an image. The features are extracted by applying Tetrolet and DWT functions like Biorthogonal 3.5, Coiflets 3, Daubechies 4, Haar, and Symlet 3 for extracting coefficients to obtain the texture information of the skin cancer images.

Extracted coefficients are sorted in ascending order out of which top 10% are considered. Features such as texture and shape are extracted from the images. Statistical texture features such as Mean, Standard Deviation, Kurtosis, skewness are calculated from the coefficients of the transform as shown in Table II.

The features such as Homogeneity, Energy and Entropy are calculated from the Gray level co-occurrence matrix as shown in Table III. The Gray level co-occurrence matrix is denoted by G(i,j). Shape features such as Area, Perimeter, Form factor, Minor Axis length and Major Axis Length are obtained from the shapes of the tumours using region growing technique. The different shapes extracted using region growing technique for Benign and Malignant dermoscopic images of the ISIC Archive are as shown in Fig. 8 and 9.

The standardization of features is done using z-score since the feature set has mix of both positive and negative values. The standardized features are given as an input to the classifier.

3) Classification: Features extracted from the skin cancer are given as an input to the K-Nearest Neighbor Classifier. KNN estimates the class of a new object based on the classes of its K Nearest Neighbors. KNN is a statistical method used for classification. In this method the Euclidean distance between feature vector of the test and the training images are calculated by considering benign and malignant images. The KNN algorithm accuracy depends on noise and unwanted features. Coefficients calculated from different skin cancer images using different wavelet functions are used to calculate the statistical texture features.

Statistical feature vector of a test image is given and Euclidean distance is measured between the test and training image set. Therefore, the distances are sorted in ascending order. Here the image with shortest distance is treated as reference image. Based on this image the test sample can be predicted. Cross validation is used to evaluate the classification accuracy for different transforms. The extracted coefficients are divided into 80% of data as training data and 20% as testing data to evaluate the overall performance.

4) Experimental Results: The statistical texture features obtained for Malignant and benign images are depicted in Tables IV and V. The features such as homogeneity, energy and entropyare calculated from the GLCM for Malignant and Benign images as shown in Table VI. The shape featuresobtained for dermoscopic images are shownin Table VII. The features such as homogeneity, energy and entropy are calculated from the GLCM for Malignant and Benign images as shown in Table 5. The shape features obtained for dermoscopic images are shown in Table 6. The main objective of the study is classification of dermoscopic images using different wavelet functions like Biorthogonal, Coiflet, Daubechies, Haar, and Symlet. The entire filter set of Daubechies, Biorthogonal, Coilfet and Symmlet were used and the accuracy was found to be highest with Daubechies 2, Biorthogonal 3.1, Coiflet 1 and Symmlet 2 as shown in Table 7. The accuracy was found to be highest using Biorthogonal 3.1 among the different wavelet functions. The Sensitivity and Specificity values using different Wavelet functions and Tetrolet transform are shown in Table 8. The area under the curve using different wavelet functions is shown in Fig.10. The accuracy was found to be highest using Tetrolet transform since it can resolve the two dimension singularities better than Wavelet transform.

The classification of dermoscopic images is done by considering statistical texture features, GLCM features and shape features. The combination of all these features lead to better accuracy. The accuracy obtained using different combination of features is shown in Table X. The combination of the three features GLCM, Shape and Texture features yields better accuracy rather than the combination of other two features.

TABLE II: Statistical Texture Features

Feature	Technique Used
Mean	$\bar{x} = \frac{1}{MN}\sum_{i=1}^{M}\sum_{j=1}^{N} x_{ij}$
Standard Deviation	$\sigma = \left\{\frac{\sum_{i=1}^{M}\sum_{j=1}^{N}(x_{ij}-\bar{x})^2}{MN-1}\right\}^{\frac{1}{2}}$
Kurtosis	$Kurt = \frac{1}{\sigma^4}\left\{\frac{\sum_{i=1}^{M}\sum_{j=1}^{N}(x_{ij}-\bar{x})^4}{MN}\right\}$
Skewness	$Skew = \frac{1}{\sigma^3}\left\{\frac{\sum_{i=1}^{M}\sum_{j=1}^{N}(x_{ij}-\bar{x})^3}{MN}\right\}$

TABLE III: Features Calculated From Glcm Matrix

Feature	Technique Used
Homogeneity	$Hom = \sum_{i=0}^{N-1}\sum_{j=0}^{N-1}\frac{P(i,j)}{1+(i-j)^2}$
Energy	$Eng = \sum_{i=0}^{N-1}\sum_{j=0}^{N-1}P(i,j)^2$
Entropy	$Ent = \frac{1}{MN}\left\{\sum_{i=1}^{M}\sum_{j=1}^{N}(x_{ij}-\bar{x})^4\right\}$

Published By:
Blue Eyes Intelligence Engineering
and Sciences Publication (BEIESP)

TABLE IV
Statistical Features Obtained For A Skin Tumor Using Different Wavelet Functions And Tetrolet Transforms

Malignant(ISIC_0000013)					
Transform	Mean	Standard deviation	Smoothness index	Skweness	Sensitivity
Haar	1.4291	0.5625	0.2404	1.3167	2.9620
Daubechies 2	1.4323	0.5617	0.2398	1.3270	2.9927
Biorthogonal 3.1	1.4334	0.5632	0.2408	1.3194	2.9907
Coiflet 1	1.4353	0.5606	0.2391	1.3373	3.0234
Symmlet 2	1.4323	0.5617	0.2398	1.3270	2.9927
Tetrolet	2.8582	1.1239	0.5581	1.3151	2.9562

TABLE V : Statistical Features Obtained For A Skin Tumor Using Different Wavelet Functions And Tetrolet Transforms

Benign(ISIC_0000000)					
Transform	Mean	Standard deviation	Smoothness index	Skweness	Sensitivity
Haar	1.2384	0.5432	0.2278	0.5968	1.6591
Daubechies 2	1.2430	0.5437	0.2282	0.6055	1.6741
Biorthogonal 3.1	1.2443	0.5462	0.2297	0.5920	1.6900
Coiflet 1	1.2471	0.5436	0.2281	0.6159	1.6885
Symmlet 2	1.2430	0.5437	0.2282	0.6055	1.6741
Tetrolet	2.4769	1.0853	0.5408	0.5953	1.6532

TABLE VI : Features Obtained For A Malignant And Benign Tumor Using Gray Levelco-Occurrence Matrix

	Malignant			Benign		
Feature	ISIC_0000013	ISIC_0000022	ISIC_0000198	ISIC_0000066	ISIC_0000101	ISIC_0009973
Homogenity	0.2404	0.0462	0.1308	0.2278	0.2060	0.1080
Energy	1.3167	1.2219	0.9696	0.5968	0.5838	1.3080
Entropy	2.9620	3.4667	2.7936	1.6591	2.4023	3.2070

TABLE VII : Shape Features Obtained For A Malignant And Benign Tumor

	Malignant			Benign		
Feature	ISIC_0000013	ISIC_0000078	ISIC_0000155	ISIC_0000000	ISIC_0000001	ISIC_0000008
Area	118401	141631	99347	155528	104299	144785
Perimeter	4689	5161	4023	4852	4305	4829
Form Factor	0.067671	0.066819	0.077137	0.083019	0.07072	0.078022
Minor Axis Length	4731022	5297220	4066436	4940563	4376956	4920450
Major Axis Length	0.9749	0.973263	0.975569	0.96852	0.96171	0.970575

Published By:
Blue Eyes Intelligence Engineering
and Sciences Publication (BEIESP)

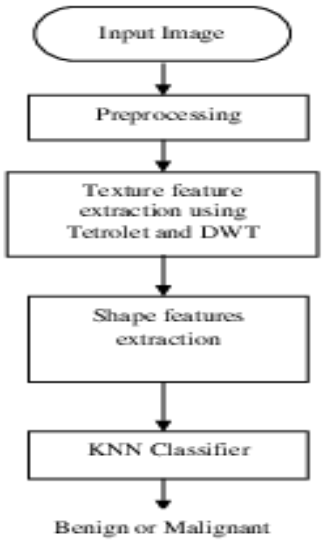

Fig 6. Methodology for detection of malignant tumors.

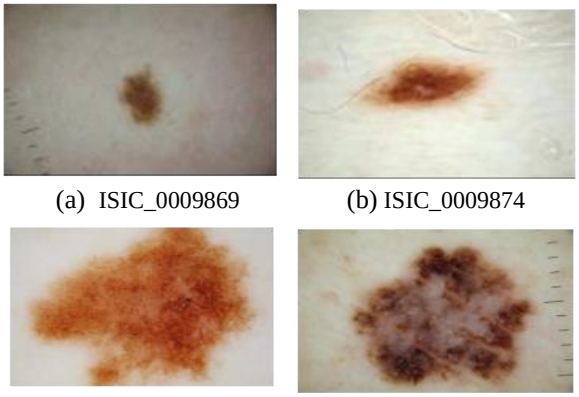

Fig 7 Dermoscopic images from ISIC database
(a),(b) Malignant images, (c),(d) Benign images

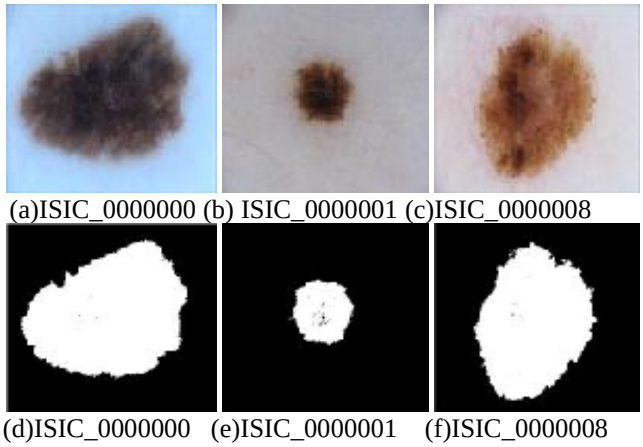

Fig 8.Shapes obtained for benign images from ISIC database using region growing technique
(a),(b),(c) Benign Images, (d),(e),(f) Shapes of Benign images

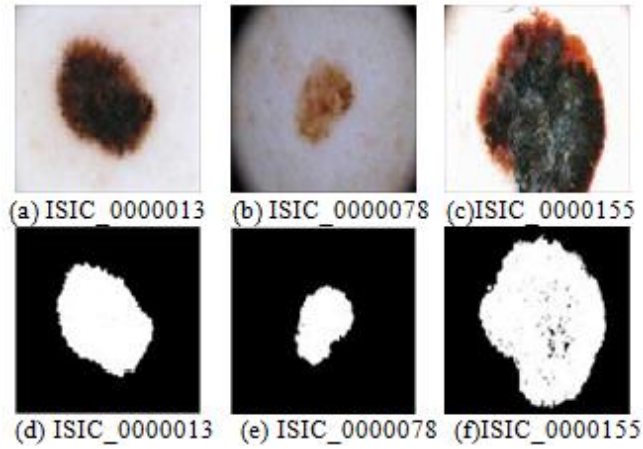

Fig 9. Shapes obtained for Malignant images from ISIC database using Region growing technique.
(a),(b),(c) Malignant images, (d),(e),(f) Shapes of malignant images

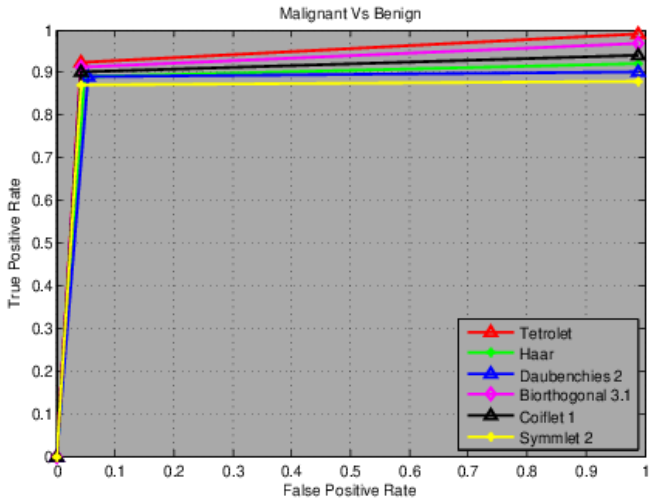

Fig 10. Area under the curve obtained using different wavelet functions

TABLE VIII :
Classification Accuracy For Classifying Benign And Malignant Tumors Of Isic Database

Transform	Accuracy
Haar	91.4012%
Daubechies2	91.2961%
Biorthogonal 3.1	91.6355%
Coiflet 1	91.3978%
Symmlet 2	91.1981%
Tetrolet	92.3478%

Published By:
Blue Eyes Intelligence Engineering and Sciences Publication (BEIESP)

TABLE IX
Sensitivity And Specificity Values Obtained Using Wavelet And Tetrolet Transforms

Transform	Sensitivity	Specificity
Haar	0.8954%	0.9142%
Daubechies2	0.8712%	0.8965%
Biorthogonal 3.1	0.9023%	0.9141%
Coiflet 1	0.8656%	0.8812%
Symmlet 2	0.8845%	0.9023%
Tetrolet	0.9142%	0.9345%

TABLE X
Performance Of Different Features For Classifying Benign And Malignant Tumors

Transform	Accuracy
GLCM+Shape+Texture	91.9355%
GLCM + Texture	88.7097%
GLCM + Shape	90.8672%
Shape+ Texture	91.3978%

A.Conclusion

This research work aims on classification of Dermoscopic images using Wavelet and Tetrolet transforms. Features such as texture, shape and GLCM are calculated from dermoscopic images. The features extracted are classified using KNN classifier. The accuracy is high using Tetrolet transform compared to other Wavelet functions. Dermoscopic images can be further classified for further detection of melanoma using other wavelet based transforms. The accuracy can be also be improved using various optimization techniques.

ACKNOWLEDGMENT

The author thank the ISIC Archive for providing skin cancer images for the present work

CONFLICTS OF INTEREST

The author has no conflict of interest with the material provided in the paper.

REFERENCES

1. http://www.skincancer.org/skin-cancer-information/skin-cancer-facts.
2. Sheha, Mariam A., Mai S. Mabrouk, and Amr Sharawy. "Automatic detection of melanoma skin cancer using texture analysis." International Journal of Computer Applications 42.20 (2012): 22-26.
3. Dobrescu, Radu, et al. "Medical images classification for skin cancer diagnosis based on combined texture and fractal analysis." WISEAS Transactions on Biology and Biomedicine 7.3 (2010): 223-232.
4. Celebi, M. Emre, et al. "A methodological approach to the classification of dermoscopy images." Computerized Medical Imaging and Graphics 31.6 (2007): 362-373.
5. Lau, Ho Tak, and Adel Al-Jumaily. "Automatically early detection of skin cancer: Study based on nueral netwok classification." Soft Computing and Pattern Recognition, 2009. SOCPAR'09. International Conference of. IEEE, 2009.
6. Elgamal, Mahmoud. "Automatic skin cancer images classification." IJACSA) International Journal of Advanced Computer Science and Applications 4.3 (2013): 287-294..
7. Yuan, Xiaojing, et al. "SVM-based texture classification and application to early melanoma detection." Engineering in Medicine and Biology Society, 2006. EMBS'06. 28th Annual International Conference of the IEEE. IEEE, 2006.
8. Yu, Lequan, et al. "Automated melanoma recognition in dermoscopy images via very deep residual networks." IEEE transactions on medical imaging 36.4 (2017): 994-1004.
9. https://isic-archive.com.
10. Krommweh, Jens. "Tetrolet transform: A new adaptive Haar wavelet algorithm for sparse image representation." Journal of Visual Communication and Image Representation 21.4 (2010): 364-374J. Jones. (1991, May 10). Networks (2nd ed.) [Online]. Available: http://www.atm.com
11. (Haenssle, H. A., et al. "Man against machine: diagnostic performance of a deep learning convolutional neural network for dermoscopic melanoma recognition in comparison to 58 dermatologists." Annals of Oncology (2018).
12. Bi, Lei, et al. "Dermoscopic image segmentation via multi-stage fully convolutional networks." IEEE Trans. Biomed. Eng 64.9 (2017): 2065-2074.
13. Rahman, Mahmudur, Nuh Alpaslan, and Prabir Bhattacharya. "Developing a retrieval based diagnostic aid for automated melanoma recognition of dermoscopic images." 2016 IEEE Applied Imagery Pattern Recognition Workshop (AIPR). IEEE, 2016
14. Sultana, Nazneen N., and N. B. Puhan. "Recent Deep Learning Methods for Melanoma Detection: A Review." International Conference on Mathematics and Computing. Springer, Singapore, 2018.
15. Adria Romero,Lopez et al. "Skin lesion classification from dermoscopic images using deep learning techniques." Biomedical Engineering (BioMed), 2017 13th IASTED International Conference on. IEEE, 2017.
16. Codella, Noel, et al. "Deep learning, sparse coding, and SVM for melanoma recognition in dermoscopy images." International Workshop on Machine Learning in Medical Imaging. Springer, Cham, 2015.
17. Yu, Lequan, et al. "Automated melanoma recognition in dermoscopy images via very deep residual networks." IEEE transactions on medical imaging 36.4 (2017): 994-1004.
18. Oliveira, Roberta B., Aledir S. Pereira, and JoÃ£o Manuel RS Tavares. "Skin lesion computational diagnosis of dermoscopic images: Ensemble models based on input feature manipulation." Computer methods and programs in biomedicine 149 (2017): 43-53.
19. Yi, Xin, Ekta Walia, and Paul Babyn. "Unsupervised and semi-supervised learning with Categorical Generative Adversarial Networks assisted by Wasserstein distance for dermoscopy image Classification." arXiv preprint arXiv:1804.03700 (2018).
20. Castillejos-FernÃ¡ndez, Heydy, et al. "An Intelligent System for the Diagnosis of Skin Cancer on Digital Images taken with Dermoscopy." Acta Polytechnica Hungarica 14.3 (2017).
21. Majtner, Tomas, Sule Yildirim-Yayilgan, and Jon Yngve Hardeberg. "Combining deep learning and hand-crafted features for skin lesion classification." Image Processing Theory Tools and Applications (IPTA), 2016 6th International Conference on. IEEE, 2016

AUTHORS PROFILE

K.S Rajasekhar, M.Tech(Embedded Systems) working as assistant professor in Acharya Nagarjuna University, Currently doing research work in the area of image processing,

Dr T. Rangababu M.Tech, PhD, professor and H.O.D ECE department in RVR & JC College of Engg & Technology, Guntur.

Published By:
Blue Eyes Intelligence Engineering and Sciences Publication (BEIESP)